Informatics in Medicine Unlocked 36 (2023) 101126

Contents lists available at ScienceDirect

Informatics in Medicine Unlocked

journal homepage: www.elsevier.com/locate/imu

In silico identification of chemical compounds in *Spondias mombin* targeting aldose reductase and glycogen synthase kinase 3β to abate diabetes mellitus

B.O. Ajiboye [a,b,*], T.M. Fagbola [c], I.M. Folorunso [d], A.W. Salami [a], O.N. Aletile [a], B.A. Akomolede [a], F.I. Ayemoni [a], K.I. Akinfemiwa [a], V.O. Anwo [a], M.I. Ojeleke [a], B.E. Oyinloye [b,e,f]

[a] Phytomedicine and Molecular Toxicology Research Laboratory, Department of Biochemistry, Federal University Oye-Ekiti, Nigeria
[b] Institute of Drug Research and Development, SE Bogoro Center, Afe Babalola University, PMB 5454, Ado, Ekiti, 360001, Nigeria
[c] Department of Computer Science, Faculty of Science, Federal University Oye-Ekiti, PMB 373, Oye, Ekiti, Nigeria
[d] Department of Biochemistry, Federal University of Technology Akure, Nigeria
[e] Phytomedicine, Biochemical Toxicology and Biotechnology Research Laboratories, Department of Biochemistry, College of Sciences, Afe Babalola University, PMB 5454, Ado-Ekiti, 360001, Nigeria
[f] Biotechnology and Structural Biology (BSB) Group, Department of Biochemistry and Microbiology, University of Zululand, KwaDlangezwa, 3886, South Africa

ARTICLE INFO

Keywords:
Diabetes
Aldose reductase
Glycogen synthase 3β
Molecular docking
Drug candidate
Drug discovery

ABSTRACT

Aldose reductase and glycogen synthase kinase 3β (GSK3β) represent two of the ideal drug targets in diabetes due to their role in the pathogenesis of diabetes. Studies have shown that plant compounds provide therapeutics in diabetes management. This study identified some compounds in *S. mombin* as dual inhibitors of aldose reductase and GSK3β. *S. mombin* compounds (n = 100) were docked with both aldose reductase and GSK3β; and the nine top scoring compounds were identified. The plant compounds were further investigated with MM-GBSA, ADME, HOMO/LUMO and constructed QSAR model to determine its stability with the targets, evaluate its drug-likeness, identify reactive molecules and predict its bioactivities against the proteins. The results show that the nine-top scoring compounds (Quercetin, Catechin, Ellagic acid, Tangeretin, Estradiol, Epicatechin, linalool, 2-Nitroethyl benzene, and Eugenol) attained stability with the proteins, and they also demonstrated excellent drug-like and pharmacokinetic characteristics, which qualifies them as drug candidates. The results identified linalool as the most reactive compound and Catechin as the most chemically inert molecules among the leads. The constructed QSAR model validated the molecular docking results by predicting satisfactory biological activities of the plant compounds against both targets. Although, the current findings have identified *S. mombin* compounds as dual inhibitors of aldose reductase and GSK3β, experimental studies are ongoing to validate the findings made by this study.

1. Introduction

Diabetes mellitus (DM) incidence is growing as a result of the epidemiologic change occurring throughout the developing countries [1]. In 2021, 537 million persons had diabetes. Diabetes is expected to affect up to 650 million individuals by 2030 and 783 million by the mid-2040s. More than three-quarters of people with diabetes are found in developing nations. Nearly one-half of all persons (240 million) with diabetes have never been properly diagnosed. In Nigeria, the current prevalence of diabetes mellitus is estimated to be 1.7% among persons aged 20–69 years [2]. It is commonly believed that the IDF's prevalence estimates drastically underestimate the real burden of diabetes mellitus in Nigeria, as they are produced by the extrapolation of data from other countries. In recent years, many researchers found incidence rates ranging from 2% to 12% across the country [3].

Diabetes Mellitus (DM) is a metabolic condition defined by insulin

* Corresponding author. Phytomedicine and Molecular Toxicology Research Laboratory, Department of Biochemistry, Federal University Oye-Ekiti, PMB 373, Oye, Ekiti, 371104, Nigeria.

E-mail addresses: bash1428@yahoo.co.uk (B.O. Ajiboye), temitayo.fagbola@fuoye.edu.ng, tunji4reele@yahoo.com (T.M. Fagbola), folorunsoim@futa.edu.ng, idowuflorence805@gmail.com (I.M. Folorunso), salamiwahley@gmail.com (A.W. Salami), oluwaseunaletile@gmail.com (O.N. Aletile), akinfemiwakehinde1999@gmail.com (K.I. Akinfemiwa), anwovictor200@gmail.com (V.O. Anwo), ojelekemercy@gmail.com (M.I. Ojeleke), blessingakomolede043@gmail.com (B.E. Oyinloye).

https://doi.org/10.1016/j.imu.2022.101126
Received 7 October 2022; Received in revised form 31 October 2022; Accepted 1 November 2022
Available online 11 November 2022

Table 1
Docking and post docking results.

s/n	Compound name	Aldose reductase					Glycogen synthase kinase 3β				
		Docking score	Intermolecular Interactions	No of H-bond	Binding free energy	pIC50	Docking score	Intermolecular Interactions	No of H-bond	Binding free energy	pIC50
1	Quercetin	−12.370	TRP111, TRP79	–	−36.48	5.742	−12.185	ASN64, ASP133, VAL135	4 Hbond	−50.49	6.120
2	Catechin	−12.119	TRP11, TRP11	–	−42.89	5.774	−10.431	ASN64, ASN186, PRO136, VAL135	4 Hbond	−42.21	5.709
3	Ellagic acid	−10.937	ALA299	1 Hbond	−33.16	6.105	−11.317	VAL135	1 Hbond	−57.67	5.887
4	Tangeretin	−10.427	TRP11, HIP110, TRP20	1 Hbond	−33.22	5.521	−9.221	ASP133, VAL135	2 Hbond	−43.56	6.271
5	Estradiol	−8.954	TRP111	–	−14.43	5.748	−8.333	–	–	−58.38	6.158
6	Epicatechin	−7.823	TRP111	–	−7.78	5.830	−8.315	TYR134	1 Hbond	−27.3	5.619
7	linalool	−5.205	TRP111, PHE122, HIP110	–	−6.74	6.025	−8.000	ILE62, ARG141	1 Hbond	−6.31	5.179
8	(2-Nitroethyl) benzene	−10.794	TRP111, ALA299	1 Hbond	−20.77	6.004	−9.150	VAL135, PRO136, ILE62	3 Hbond	−37.33	4.984
9	Eugenol	−6.757	THR113, TRP111	–	−32.65	6.121	−8.854	VAL135	1 Hbond	−35.04	6.094
10	CO-LIGAND	−10.085	TRP111, H1P110, THR113, TYR48	5Hbond	−66.7	6.654	−10.306	VAL135, ASP133, ASP200	4 Hbond	−73.92	6.376

deficiency and decreased tissue sensitivity to its actions; and hypoinsulinemia and hyperglycemia are the two most prominent clinical manifestations of diabetes. Two common types of DM are known namely; type 1 diabetes mellitus (type 1 DM) and type 2 diabetes mellitus (Type 2 DM), with the later accounting for more than 90% of diabetes related cases [4]. Type 1 DM is caused by autoimmune destruction of insulin secreting cells. Type 2 DM is mediated by resistance to insulin action caused by fewer working insulin receptors, stress, and medications [5]. Acute clinical manifestations of diabetes are but not limited to polyuria, increased thirst, dehydration, electrolyte abnormalities, weight loss, and metabolic decompensation, which includes diabetic ketoacidosis and non-ketotic hyperosmolar coma [6]. Retinopathy, nephropathy, and neuropathy are long-lasting effects of the disease [7]. The severity of acute and chronic effects is inversely proportional to the level of metabolic regulation. These fundamental principles serve as the foundation for understanding the origins, pathophysiology, classification, and diagnosis of diabetes.

The polyol pathway is a critical method through which elevated glucose levels can cause oxidative stress to emerge [8,9]. The first step in the polyol pathway, which transforms glucose into sorbitol, is catalyzed by aldose reductase (AR), an aldo-keto reductase [10]. Using AR defective mice, previous investigations have revealed that the polyol pathway is a major source of diabetes-induced oxidative stress [11,12]. The polyol pathway may contribute to oxidative stress in one of three ways. The first mechanism takes place during hyperglycemia where about one-third of the glucose is directed to AR-dependent polyol pathway depleting NADPH and lowering GSH [8]. Secondly, the SDH conversion of sorbitol to fructose causes oxidative stress in the cells (i.e., the second step of polyol pathway). NAD^+ is transformed into NADH by the SDH in this phase. In the presence of NADH, the enzyme NADH oxidase generates superoxide anions [10]. A third non-enzymatic glycation agent is produced from glucose via the polyol pathway, and this fructose can be further converted into fructose-3-phosphate and 3-deoxyglucosone. Because glucose is moving faster via the polyol route, advanced glycation end-products (AGEs) are being formed, which leads to the creation of ROS. Hence, AR has been a focus of intense research as a vital target for preventing and controlling diabetic complications, with the hope that inhibiting AR might be an effective strategy for preventing or delaying diabetes problems [13].

Glycogen synthase kinase 3β, a serine/threonine protein kinase, is an isoform of GSK-3 that affects the function of several metabolic, signaling and structural proteins through mediation of phosphates on to serine and theronine amino acid residues. Due to its pivotal role in the onset and progression of diseases including diabetes mellitus, GSK-3β has recently been a subject of much research in recent years [14]. Insulin signaling can acutely inactivate GSK3β by activating IRS-1, PI3-kinase, and finally Akt to phosphorylate particular serine residues on the enzyme. The same time courses for insulin-dependent Akt activation and GSK-3β inactivation support the idea that GSK-3β is a physiologically relevant Akt substrate [15]. GSK3 also phosphorylates IRS-1 on serine and threonine residues, impairing insulin signaling [16]. These findings support the idea that GSK3β can inhibit insulin effect on glycogen synthase and possibly glucose transport. GSK3β inhibitors have been demonstrated to increase glucose tolerance and insulin sensitivity in multiple investigations using diabetic models [17]. Selectivity is a serious challenge when using GSK3 inhibitors to demonstrate GSK-3 participation in cellular processes; many GSK3 inhibitors have low selectivity based on limited kinase panel testing [18].

This current study identifies the chemical constituents in *Spondias mombin* as potential inhibitors of AR and GSK-3β to abate diabetes mellitus related complications. Spondias mombin L. is a plant member of Anacardiaceae family. It is common throughout tropical areas of America, Africa, and Asia [19]. *S. mombin* is a medicinal plant used in folk medicine to prevent and treat diabetes amongst other diseases, especially in the Western part of Nigeria. Studies have demonstrated its anti-diabetic properties owing to its hypoglycemic effects. This plant has been documented to have different phytochemicals by series of scientists, (e.g. phenolic acids, flavonoids, tannins, triterpenes, etc. have been isolated from S. mombin) among them is [19,20]; etc. Computational approaches such as molecular docking, binding free energy, ADME, QSAR and HOMO/LUMO calculations were adopted to screen the library of compounds from *S. mombin* and identify lead compounds inhibiting the activity of AR and GSK-3β.

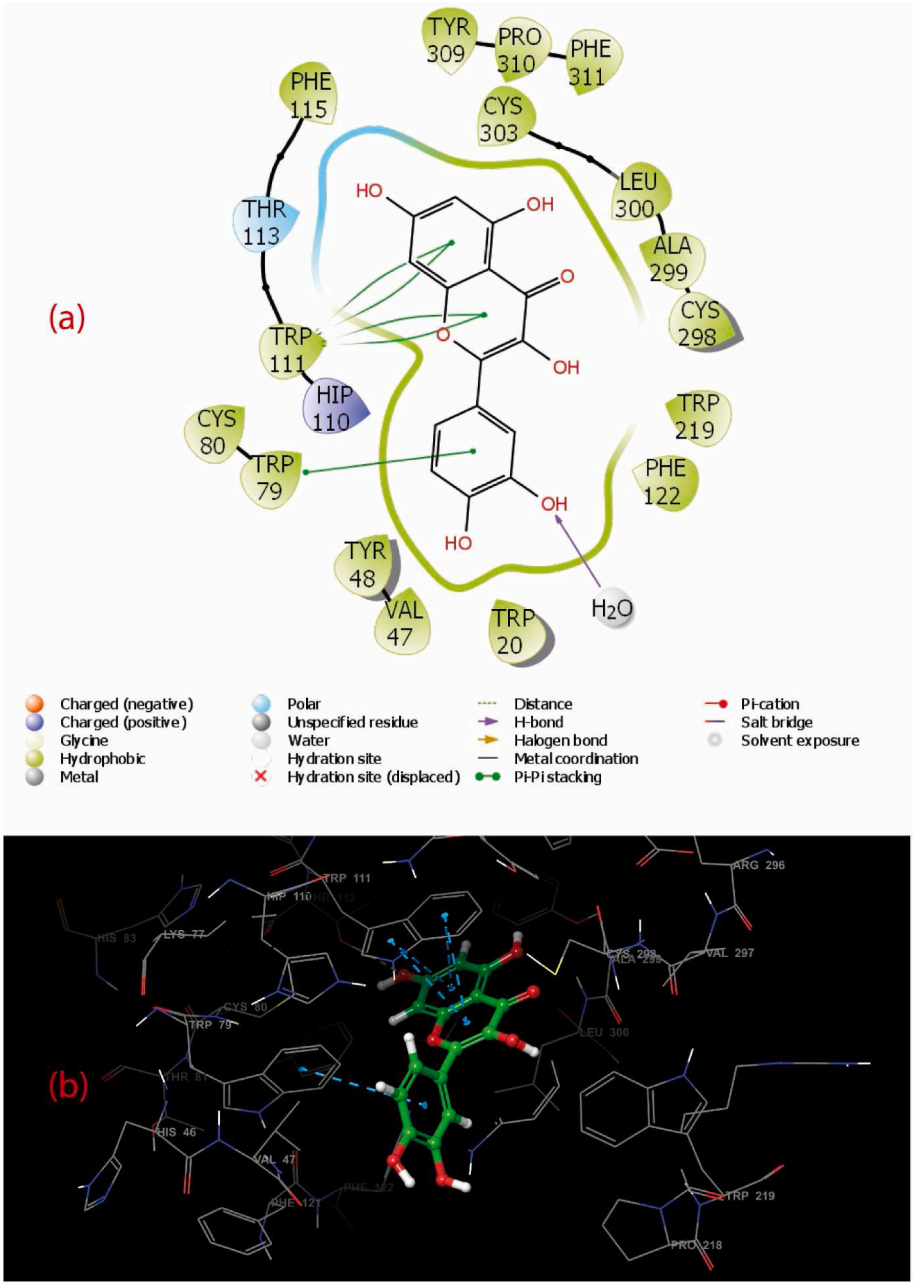

Fig. 1a. 2D and 3D plots of Quercetin interacting with amino acid residues of aldose reductase.

2. Materials and methods

2.1. Identification of the Plant's compounds, and its preparation

Through an extensive literature search, approximately one-hundred plant compounds were identified in *S. mombin*. The 2D structures of these identified phyto-compounds were downloaded from the Pubchem chemical database (SDF Format), to create a library of chemical compounds. These compounds were uploaded on Maestro graphical molecular interface, and its preparation was carried out utilizing the ligprep module of Schrodinger maestro. The compounds were optimized using OPLS3e force field, after desalting, retaining specified chiralities and adopting Epik to generate states of the chemical compounds at pH 7.0 ± 2.0.

2.2. Source of protein crystal structures and its preparation

The protein crystal structure of human glycogen synthase (GSk3β), and human aldose reductase (ALR) was sourced from protein data bank repository (http://www.rcsg.org), a database that stores 3D biological molecules, including protein and nucleic acid (wwPDB consortium, 2019). The unique identification number of these proteins are PDB ID: 1UV5 and PDB ID: 1UV5, and the binding pocket of the structures were defined because it was crystalized with ligand. The structures (PDB format) were prepared protein preparation wizard to amend common errors that accompany the structures during X-ray crystallography such as missing hydrogen bonds, water molecules that do not contribute to the activity of the protein. The OPLS3e force field was used to fill in missing residues, remove non-standard residues, optimize hydrogen

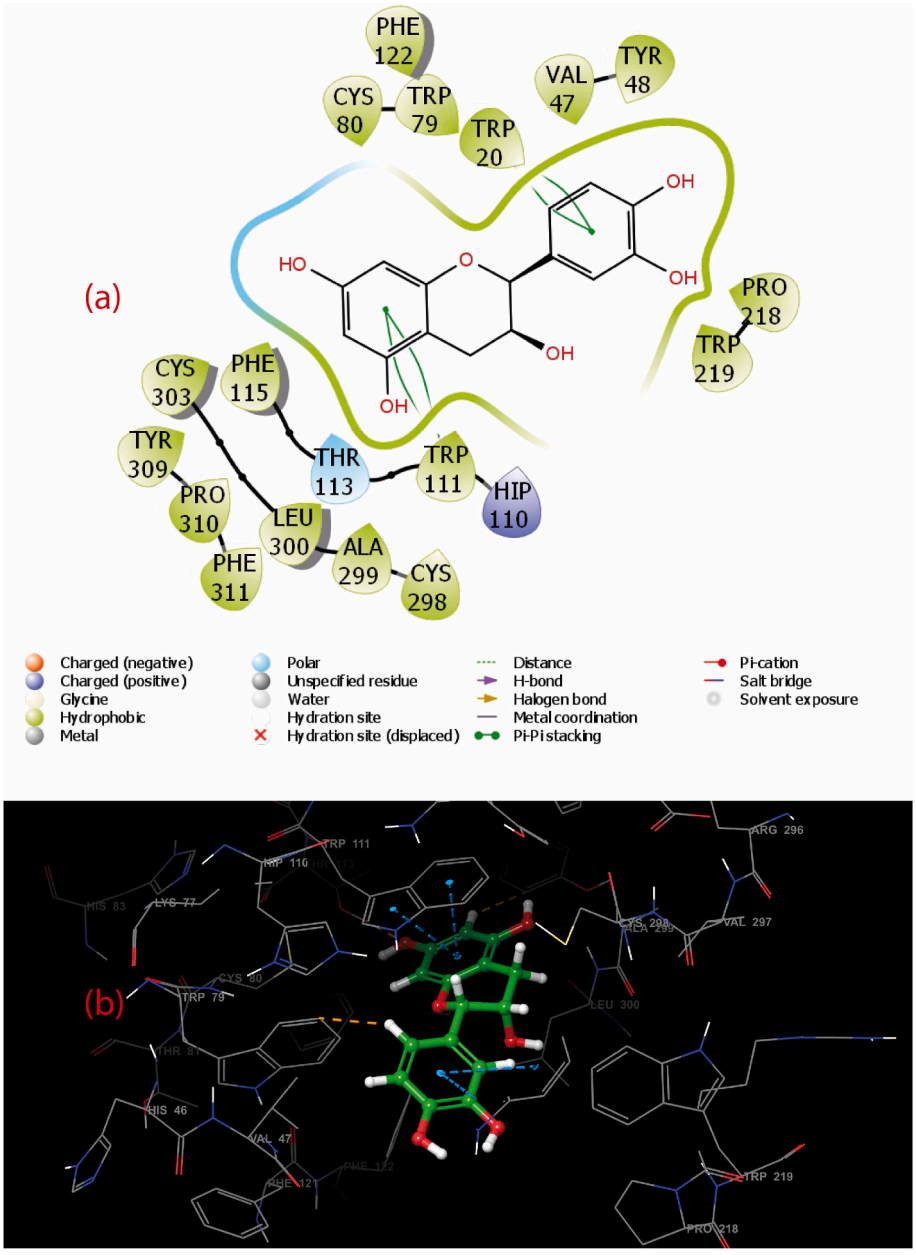

Fig. 1b. 2D and 3D plots of Catechin interacting with amino acid residues of aldose reductase.

bonding networks, remove water with less than 3 hydrogen bonds, and reduce atoms [21].

2.3. Generation of grid file to define the structures' binding pocket

The structures binding pocket was defined on receptor grid generation module by identifying the molecular (ligand) attached to the structure so as to supply the X, Y, and Z coordinates. This will enable the docked ligand confined to the supplied coordinates. The grid file of ALR had supplied coordinates of 20.95, −6.04. and 27.51 for X, Y, and Z coordinates. The coordinates describing the binding pocket of GSk3β are 93.94, 68.03 and 9.8 for X, Y, and Z site point.

2.4. Molecular docking studies

The Glide Ligand Docking panel is used to configure and execute docking activities that utilize previously computed receptor grids. HTVS docking allows fast screening of huge numbers of ligands. As opposed to docking methods, HTVS does not support score-in-place. HTVS lacks advanced options and instead uses preset values. Extra-precision (XP) docking and scoring is a more powerful and discriminating method than standard precision (SP) and HTVS, although it is more time consuming to conduct. It is intended for usage on ligand postures that have been identified to be high-scoring utilizing SP docking to be utilized with XP. After running the compounds from *S. mombin* with HTVS docking, 30 top-scoring compounds were redocked using XP, so that the more expensive docking simulation is only performed on desirable poses.

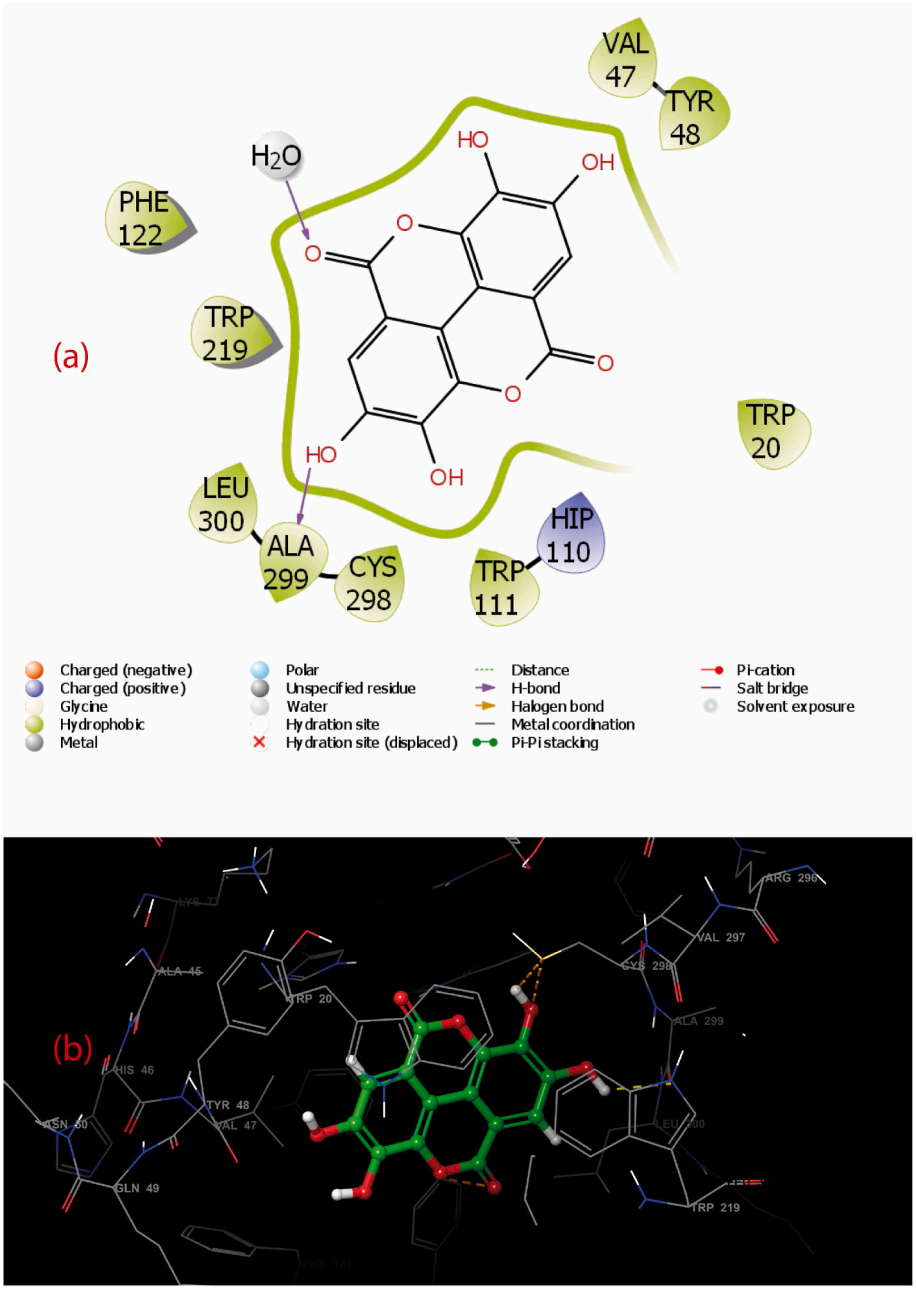

Fig. 1c. 2D and 3D plots of Ellagic acid interacting with amino acid residues of aldose reductase.

2.5. Calculated binding free energy

The stability of the ligand-bound protein was assessed in terms of binding free energy in order to determine the reliability of the protein-ligand complex output [21]. It was necessary to calculate the binding free energy using the prime MMGBSA module, which was made accessible on maestro. It is a molecular mechanics free energy technique (coupled with generalised Born and surface area continuum solvation) that calculates the free energy of a ligand to a macromolecule by calculating the free energy of the ligand to the macromolecule. According to the following equations, the primary MMGBSA determines the free energy difference between the minimised protein-ligand complex and the unbound protein and ligand:

$$E\ minimised\ complex = E\ minimised\ protein - E\ minimised\ ligand \quad ----(i)$$

2.6. ADME prediction

The drug-likeness, physicochemical properties, pharmacokinetic properties of the chemical compounds from *S. mombin* was predicted by Qikprop.

2.7. Single point calculation to determine the reactivity and inertness of compounds

The fundamental principle of the density functional theory (DFT) are derived from the Hohenberg-Kohn theorem, which asserts that the energy of a system may be expressed as a functional that is entirely dependent on the electron density. The chosen chemical compounds from *S. mombin* were geometrically optimized on jaguar fast engine on Maestro using Becke's three-parameter exchange–correlation functional hybrid (B3LYP) as a functional set and 6-31G** as a basis set, using DFT

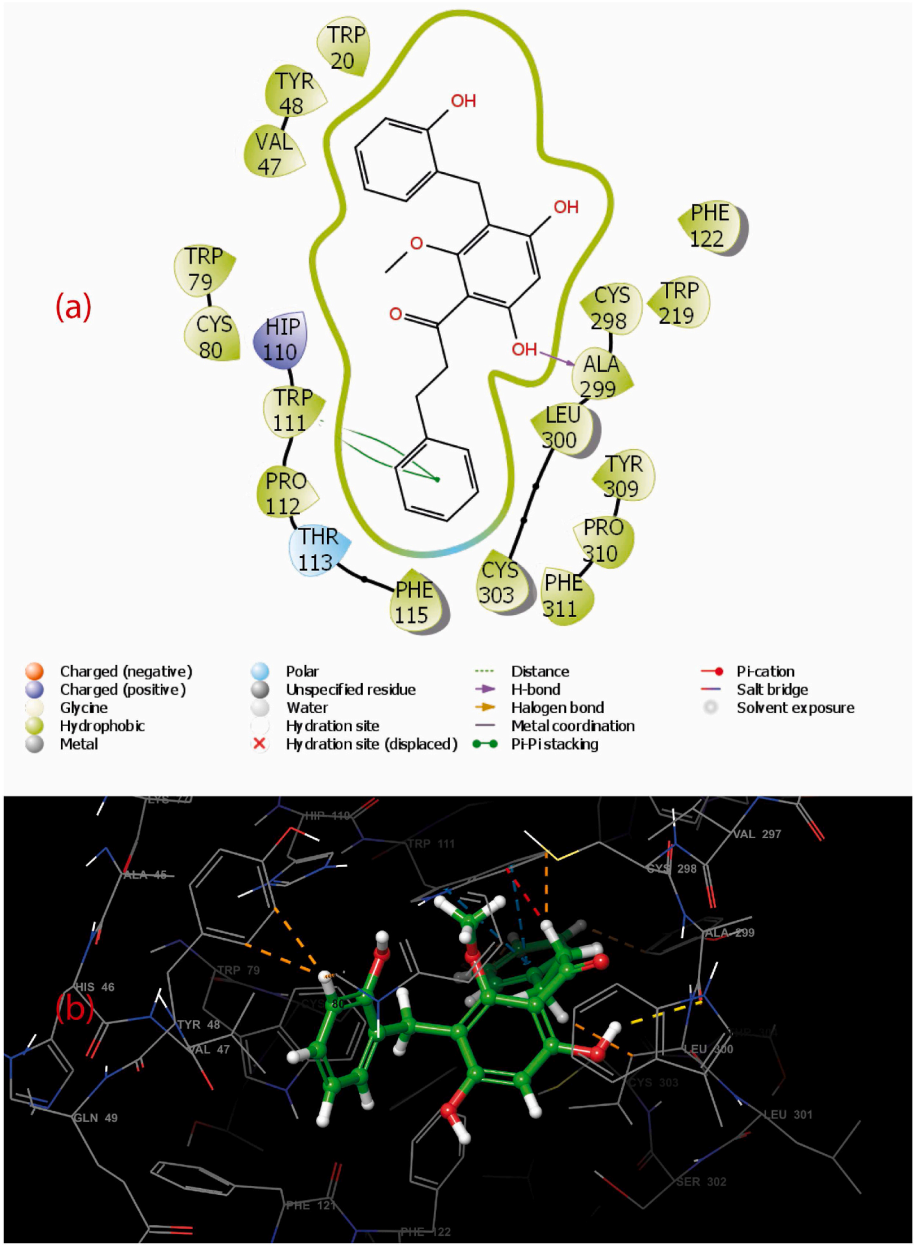

Fig. 1d. 2D and 3D plots of 2-Nitroethyl benzene interacting with amino acid residues of aldose reductase.

as level of theory. Subsequently, Surface properties of the geometrical optimized compounds which include Molecular orbitals in gas phase were calculated.

2.8. Construction of QSAR model

The retrieval of experimental compounds with established biological activities against the targeted therapeutic target is the most important criterion for developing a predictive quantitative structure activity relationship (QSAR) model for drug discovery. Thus, the chemical and bioactivity (IC50) profile of a given set of experimental data sets of GSK3β and AR from the ChEMBL database by blasting the protein FASTA sequence. The dataset were sorted out on excel sheet document to remove compounds without viable inhibition constant. The dataset containing canonical smiles of the compounds together with IC50 were converted to SDF format using Datawarrior application software. These compounds were subsequently uploaded unto maestro graphical interface, and the compounds' preparation was performed using ligprep module. The QSAR model was constructed using AutoQSAR panel, by taking into consideration the topological and physicochemical descriptors of the chemical compounds in addition to its binary fingerprints.

3. Results and discussion

This current study sort to identify the bioactive compounds in *S. mombin* as potential inhibitors of aldose reductase and glycogen synthase kinase 3β (GSK3β) using series of computational approach

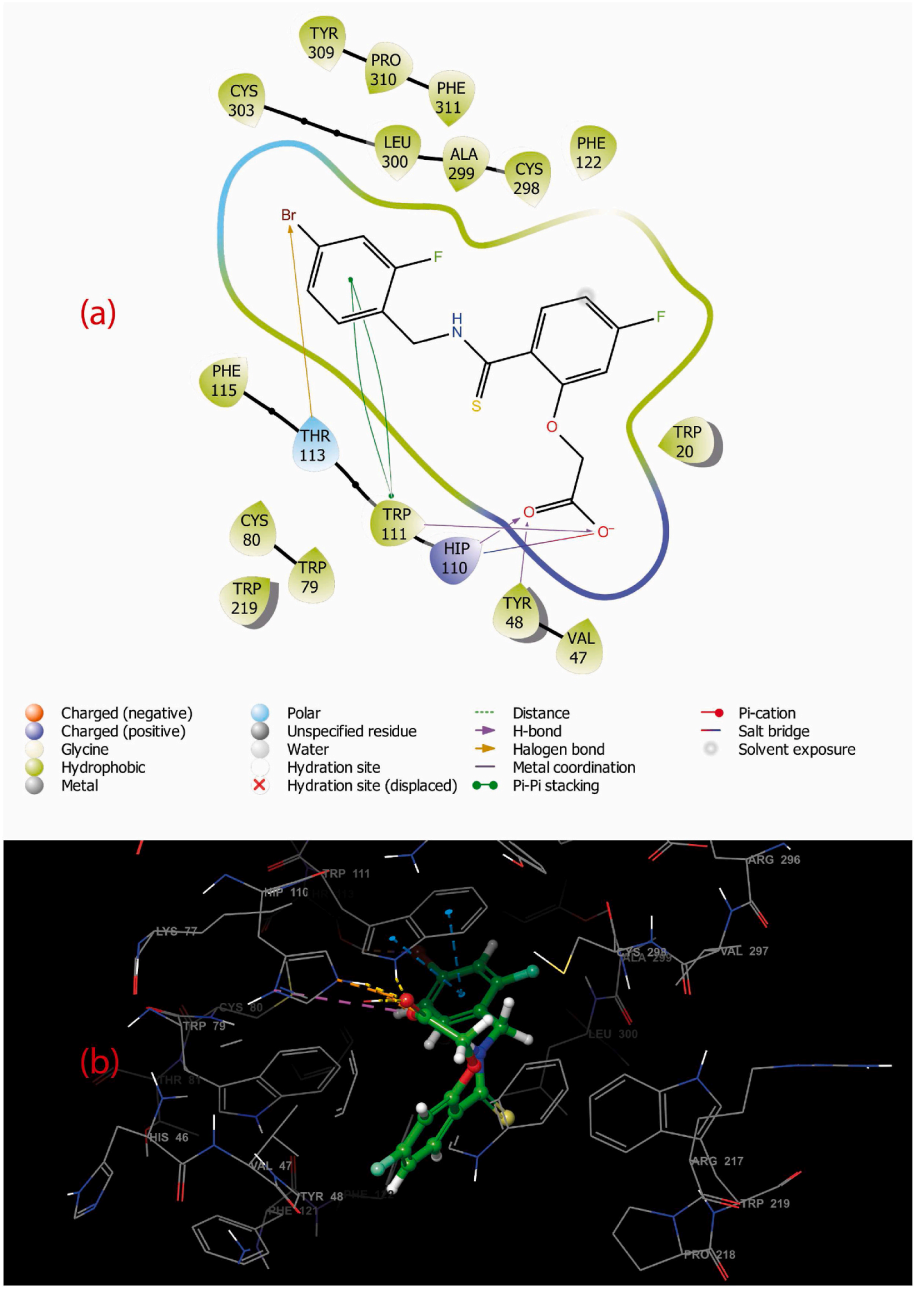

Fig. 1e. 2D and 3D plots of co-ligand interacting with amino acid residues of aldose reductase.

which includes molecular docking, binding free energy, ADME prediction, QSAR modeling and HOMO/LUMO prediction. Overall, this study identify nine compounds from *S. mombin* as leads, which showed therapeutic relevancy against aldose reductase and GSK3β; consequently, these compounds were compared with the co-ligand of these protein to established significant outcome of these research.

3.1. Molecular docking studies

The molecular docking technique is employed to simulate the atomic level interaction between a small molecule and a protein, allowing us to define the behavior of small molecules at the binding region of target proteins as well as to understand essential biochemical processes [22]. At the end of the molecular docking analysis this study identifies the following compounds with high binding affinity with both aldose reductase and GSK3β; Quercetin, Catechin, Ellagic acid, Tangeretin, Estradiol, Epicatechin, linalool, 2-Nitroethyl benzene, and Eugenol. These compounds showed a docking score of −12.370 kcal/mol, −12.119 kcal/mol, −10.937 kcal/mol, −10.427 kcla/mol, −8.954 kcal/mol, −7.823 kcal/mol, −5.205 kcal/mol, −10.794 kcal/mol and −6.757 kcal/mol with aldose reductase. However, only five of these compounds had better binding affinity with aldose reductase. The comprehensive docking results of this *in silico* experiment are given in Table 1. The docking results of these same set of compounds with GSK3β are also shown in Table 1. Quercetin, Catechin and Ellagic acid exhibited the most favorable docking score with GSK3β, and they recorded a docking score of −12.185 kcal/mol, −10.431 kcal/mol, and −11.317 kcal/mol; these results are way better than the docking score achieved by the coligand (−10.306 kcal/mol) upon binding with GSK3β. Other compounds; Tangeretin, 2-Nitroethyl benzene, Estradiol, Epicatechin, linalool, and Eugenol achieved docking scores of −9.221 kcal/mol, −9.150 kcal/mol, −8.333 kcal/mol, −8.315 kcal/mol, −8.000 kcal/mol

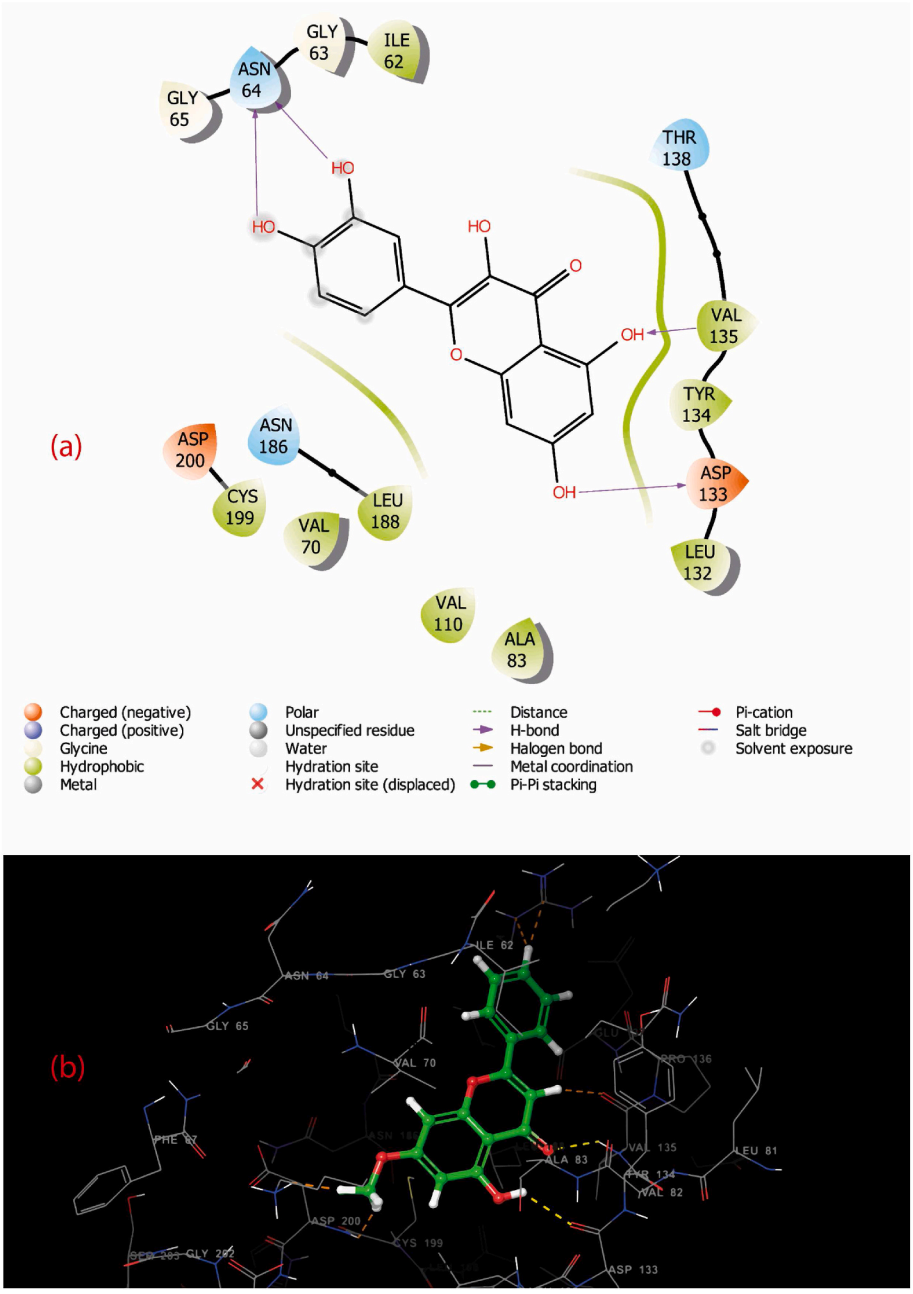

Fig. 2a. 2D and 3D plots of Quercetin interacting with amino acid residues of glycogen synthase kinase 3β.

and −8.854 kcal/mol respectively. The favorable docking results obtained by these plants compounds showed that they could modulate aldose reductase and GSK3β by inhibiting their activity.

3.2. Post-docking analysis

The post molecular docking analysis was calculated using Prime MM-GBSA; and this technique is particular important to determine the stability of the receptor-ligand complexes. It has been established in recent studies that binding free energy calculation is one of the reliable methods to validate docking score results. The binding free energy is expressed as ΔG. Mathematically, docked complexes with negative ΔG value indicate a very stable protein-ligand complex whereas, positive ΔG value equates false docking results. The binding free energy results is shown in Table 1. The nine bioactive compounds formed a stable complex with both aldose reductase and GSK3β. Quercetin, Catechin, Ellagic acid, Tangeretin, Estradiol, Epicatechin, linalool, 2-Nitroethyl benzene, and Eugenol exhibited binding free energy of −36.48 kcal/mol, −42.89 kcal/mol, −33.16 kcal/mol, −14.43 kcal/mol, −7.76 kcal/mol, −56.74 kcal/mol, −20.77 kcal/mol and −32.65 kcal/mol with aldose reductase (Table 1). The binding free energy calculations of nine bioactive compounds in complex with GSK3β are also favorable. Although the co-ligand maintained enriched high stability (−73.92 kcal/mol) with GSK3β, the other nine plant compounds had substantial native binding free energy values to justify their stability with GSK3β. The comprehensive.

3.3. The compounds interaction profiles with aldose reductase and GSK3β

After using the crystallized ligand to map the amino acid residues within the binding pocket of aldose reductase, the residues PHE115, THR111, HISP110, TRY48, VAL47, TRYP20, CYS303, TRY309, PRO310,

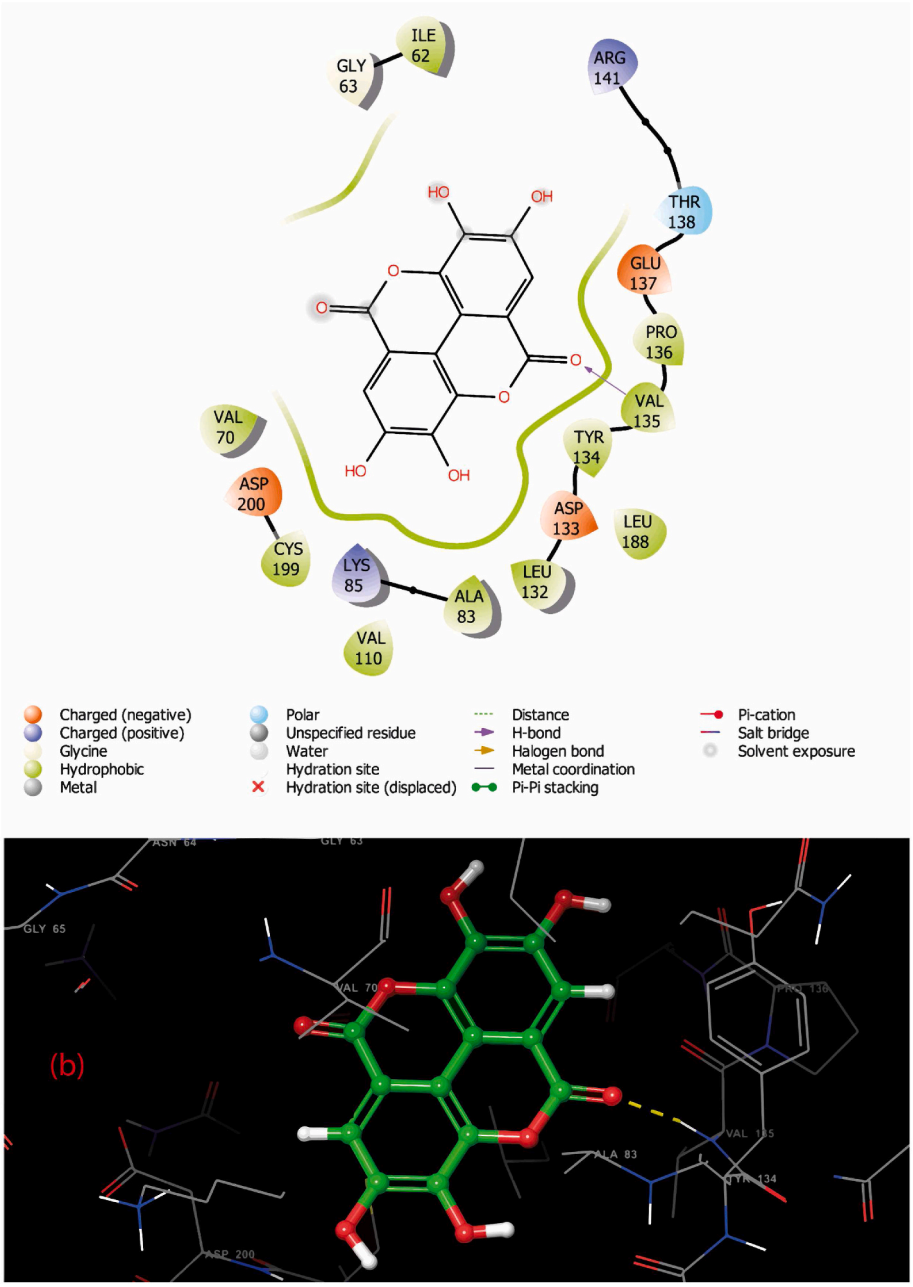

Fig. 2b. 2D and 3D plots of Ellagic acid interacting with amino acid residues of glycogen synthase kinase 3β.

PHE311, LEU300, ALA299, CYS298 and PHE112 were identified. These identified amino acids have also been well established in recent findings [23,24]. It has also been demonstrated that non-covalent interaction of small molecules with both the hydrophobic amino acids (TYR48 and TRP111) and polar amino acid (HIP110) within the catalytic cavity promote the inhibition of aldose reductase [25,26]. Consequently, the lead compounds identified in present study made pi-pi interactions or hydrogen bond interactions with the aforementioned hydrophobic and polar amino acid residues; the results are given in Table 1, while the two and three dimensional interactions of the 4 top-scoring compounds (Quercetin, Catechin, Ellagic acid and of 2-Nitroethyl benzene) and coligand are shown in Fig. 1a, b, 1c, 1d and 1e. Descriptively, the three phenyl rings of Quercetin formed pi-pi interaction with TRP111, HIP110 and TRP79; catechin made non-covalent contacts with Trp 20 and TRP111 using its phenyl ring; Ellagic acid interacted with ALA299 by forming H-bond network using one of the hydroxyl group; 2-Nitroethyl benzene formed H-bond with ALA299 and pi-pi interaction with TRP111. The coligand with rich interaction profile made H-bond network with TRP112 by interacting with bromine, TRP11 by interacting with oxygen atom, HIP110 by interacting with oxygen atom, and oxygen atom of carbonyl compound. Also, one of the phenyl ring of the coligand formed a double pi-pi interaction with TRP111. The interactions of these nine compounds from S. mombin may give insight into the mechanisms through which they inhibit aldose reductase.

Inhibition of GSK3β is an important therapeutic approach to ameliorating diabetes complications. Structurally, the binding site of GSK3β contains both the polar and hydrophobic amino acid residue. The former are known to play critical role in the ligand-ATP recognition. For example, ASP200 formed intermolecular interactions with the phosphate group of ATP. Consequently, numerous studies have identified VAL135 and ASP133 as critical residues for H-bond formation with a varied array of inhibitors [27,28], alongside GLN185, LYS183, ILE62, ASN186, and ARG141 [23]. The lead compounds identified in *S. mombin* interacted with most of these crucial residues; and the interaction profile

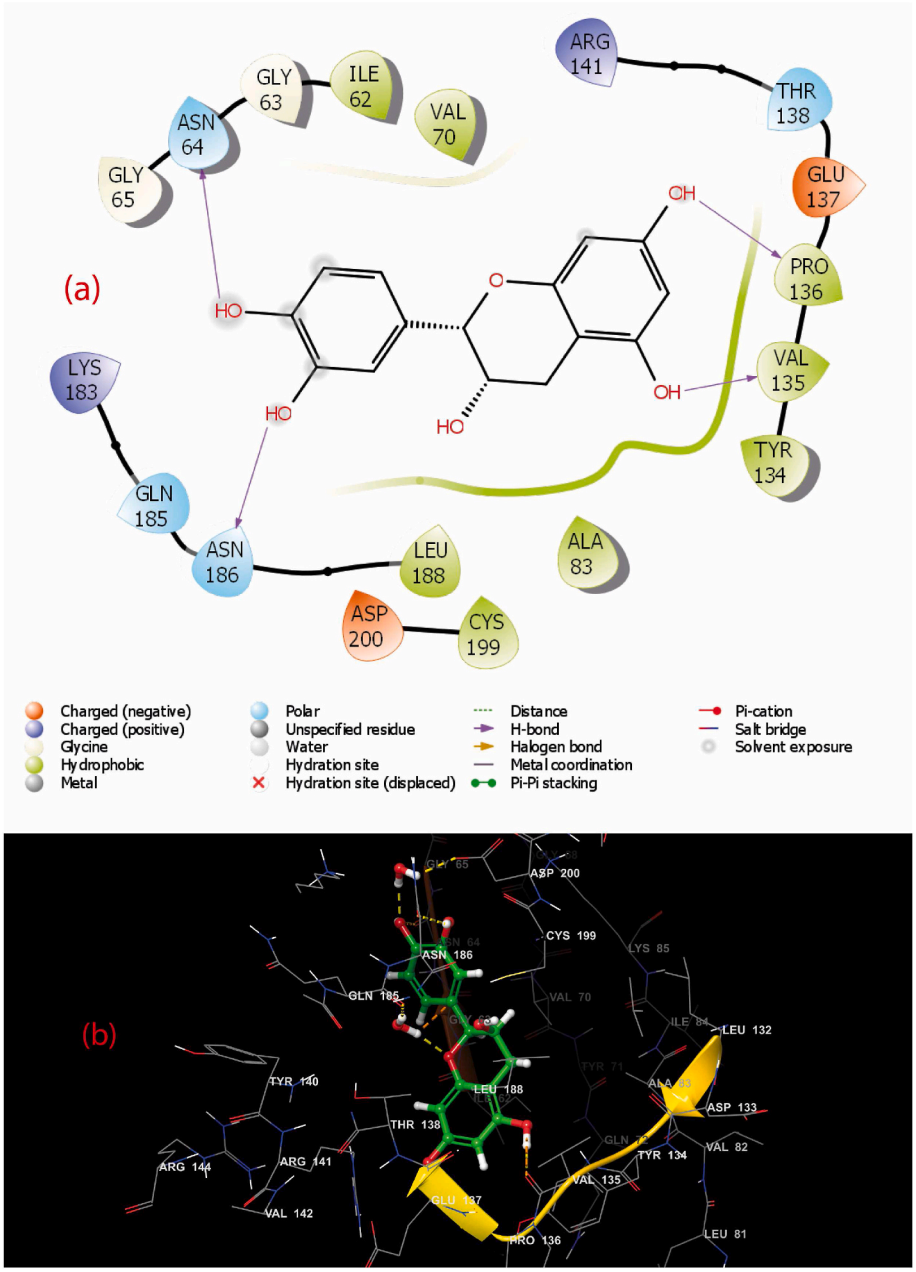

Fig. 2c. 2D and 3D plots of Catechin interacting with amino acid residues of glycogen synthase kinase 3β.

is given in Table 1. These compounds made H-bond interactions with ASN64, ASP133, VAL135, ASN186, PRO136, TYR134, ILE62 and ARG141. The interaction plot between the top 4 scoring compounds, and GSK3β are shown in Fig. 2a, b, c and d. Quercetin formed 4 H-bond interactions with ASN64, ASP133 and VAL135; Ellagic acid interacted with VAL135 using the oxygen atom of its carbonyl group; Catechin utilized its hydroxyl group to form hydrogen bonds with ASN186, PRO136, VAL135 and ASN66; and Tangeretin formed H-bond interactions with ASP133 and VAL135. The types of interaction were also demonstrated in previous study [21,23,24].

3.4. ADME prediction

Drug development is inherently tasking. The cost of developing a drug is huge, and the chances of producing therapeutic compounds with minimal toxicity are slim. Only a small fraction of lead compounds are approved by the FDA [29]. A drug lead can be canceled at any time throughout the drug development process due to ineffectiveness, side effects, toxicity, inadequate absorption, or poor clearance. Sadly, the more promising a drug lead seems, the more expensive it is to kill it. One possible path is ADME prediction or modeling (absorption, distribution, metabolism and excretion). ADME data can help forecast how a medicine will be handled or received by the body. While a pharmacological lead may be highly effective *in vitro*, bad ADME results nearly always end its development [30]. The results in Table 2 presented the parameters for drug-likeness and pharmacokinetic properties of the chemical compounds. The physicochemical properties, which shows chemical and physical properties of the compounds such as molecular weight, H-bond donor and H-bond acceptor helps to evaluate drug-likeness of the compounds. The results showed that plant compounds molecular weight, H-bond donor and H-bond acceptor, octanol/water partition coefficient (QPlogPo/w) are within the range of 164.20–402, 0 to 5, 1.5 to 8, and -1.288 to 4.526 (Table 2). These values fell within the acceptable values. The compounds are also orally available after

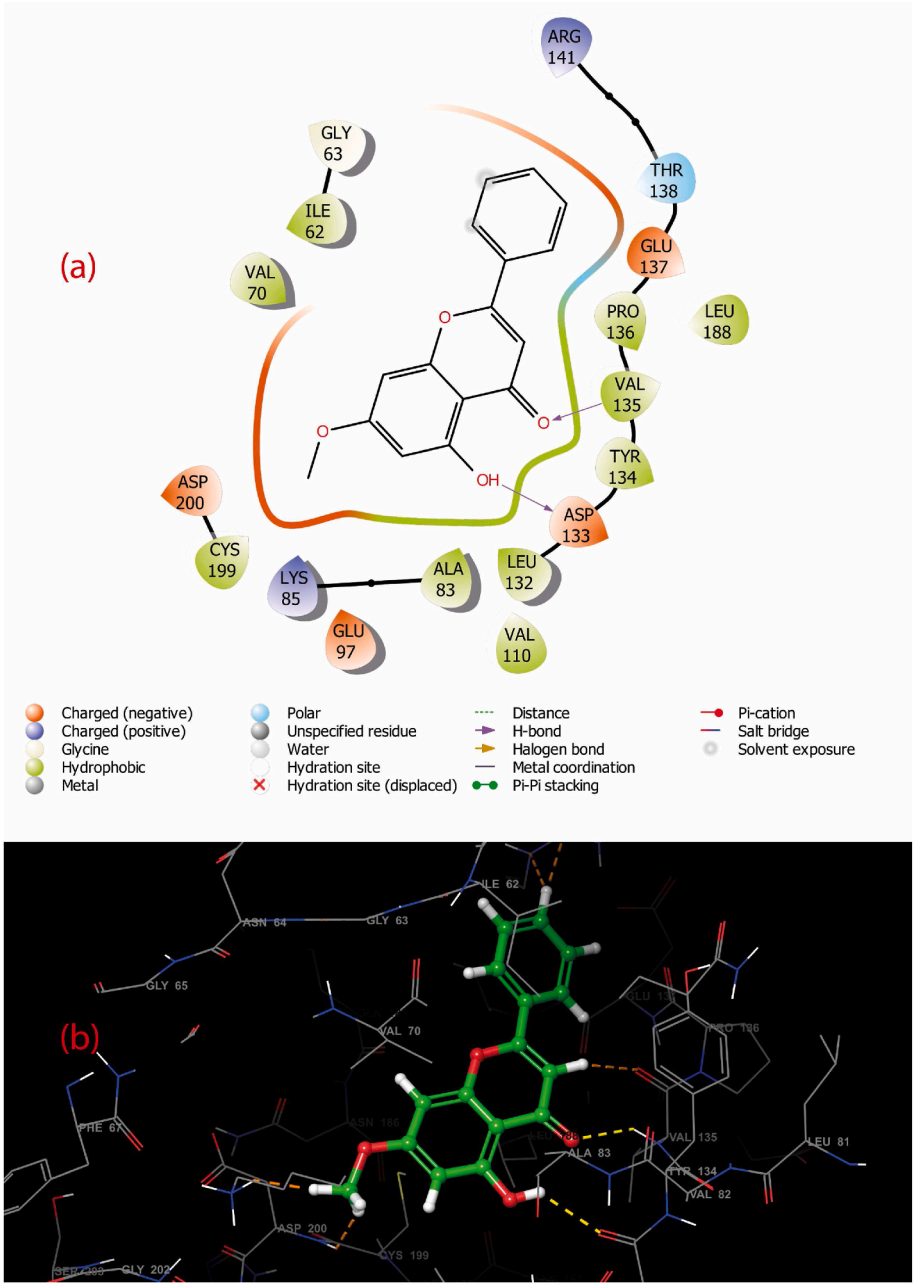

Fig. 2d. 2D and 3D plots of Tangeretin interacting with amino acid residues of glycogen synthase kinase 3β.

meeting Lipinski's rule of 5 (RO5) qualifying criteria [31]. The rule prioritize that a compound as drug candidates if it obey more than two of the following values; No more than 5 hydrogen bond donors, no more than 5 hydrogen bond acceptors, molecular weight less than 500 kDA, log P that do not exceed −5. Accordingly, all these compounds including the crystallized ligand binding to the proteins showed drug-like properties. These is further verified with the results obtained for Human oral availability (HOA). The HOA attest that the compounds had medium or high availability. This implies that these compound has high tendency to be absorbed by the gastro intestinal tract (GIT). The compounds' pharmacokinetic properties were assessed by evaluating its binding human serum albumin, blockage of HERG K+ channels, and Caco-2 cell permeability in nm/sec. The compounds' values for these parameter are within the recommended values. Hence, these compounds exhibited excellent pharmacokinetic properties, which may foster distribution of the compounds metabolites where it is needed to perform a unique pharmacological relevancy.

3.5. HOMO/LUMO calculations

Molecular orbitals with the highest occupied (HOMO) and lowest unoccupied (LUMO) energies create the frontier molecular orbital (FMO), which is critical in illustrating the active sites of compounds during molecular interactions. The HOMO and LUMO regions for the nine plants' compounds are showing in Fig. 3a and b. LUMO refers to the orbitals of a molecule that are energetically open to accepting electrons, whereas HOMO refers to the particular region in compounds with the greatest energy and most reactive electrons. Hence it has been hypothesized that bonding orbitals generated a strong link between a ligand and receptor in these locations [32]. The Compounds' HOMO/LUMO values as predicted by DFT are given in Table 3. The compounds energy level (expressed in eV) for the HOMO are between −0.22641 and −0.20055; whereas compounds energy level for the LUMO are between −0.00150 and −0.07944. These imply that Eugenol expressed the lowest HOMO while Ellagic acid had the biggest LUMO value (Table 3).

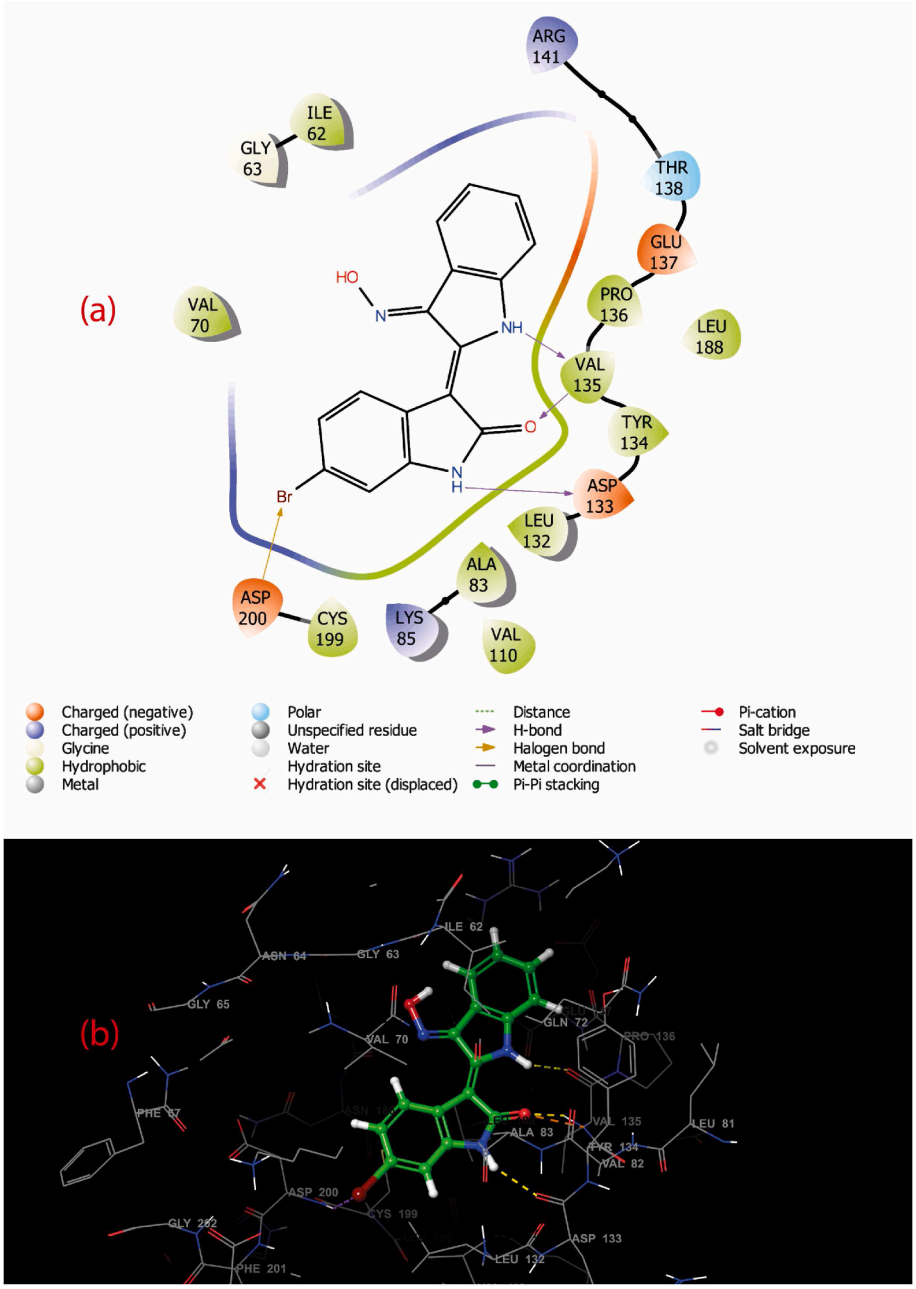

Fig. 2e. 2D and 3D plots of co-ligand interacting with amino acid residues of glycogen synthase kinase 3β.

Table 2
Physicochemical/Pharmacokinetic properties, and oral availability of the compounds.

Entry Name	[a]mol MW	[b]donorHB	[c]accptHB	[d]RuleOfFive	[e]QPlogPo/w	[f]QPlogHERG	[g]QPPCaco	[h]QPPMDCK	[i]QPlogKhsa	[j]HOA	[k]PSA
Quercetin	302.24	4	5.25	0	0.384	−4.94	21.555	7.818	−0.35	2	139.181
Ellagic acid	302.197	4	8	0	−1.288	−3.866	8.009	2.682	−0.659	2	165.005
(−)-Catechin	290.272	5	5.45	0	0.459	−4.796	57.542	22.597	−0.428	2	114.162
Tangeretin	268.268	0	3	0	3.126	−5.334	1269.14	640.076	0.209	3	63.608
(2-Nitroethyl)benzene	378.424	2	4	0	4.457	−6.158	651.474	311.311	0.571	3	88.701
Eugenol	164.204	1	1.5	0	2.673	−4.008	3039.455	1645.11	−0.102	3	29.989
Estradio	402.4	0	7	0	3.465	−4.577	3747.515	2062.997	−0.069	3	75.4
(−)-Epicatechin	272.386	2	2.45	0	4.008	−3.699	1190.401	597.263	0.458	3	44.098
Linalool	378.424	2	4	0	4.526	−6.4	647.739	309.382	0.598	3	84.725
COLIGAND-1UV5	356.178	2	4.2	0	2.598	−5.296	409.289	500.081	0.117	3	84.769
CO-LIGAND 2R24	416.237	2	4.75	0	4.511	−3.14	451.099	3251.91	0.017	3	69.25

[a] Molecular weight**; Range or recommended values -** 130.0–725.0.
[b] Hydrogen bon donor; **Range or recommended values -** 0.0–6.0.
[c] Hydrogen bond acceptor; **Range or recommended values -** 2.0–20.0.
[d] Lipinski rule of five; Number of violations of Lipinski's rule of five. The rules are: mol_MW < 500, QPlogPo/w < 5, donorHB ≤5, accptHB ≤10. Compounds that satisfy these rules are considered drug-like. (The "five" refers to the limits, which are multiples of 5.)
[e] Predicted octanol/water partition coefficient **Range or recommended values -** −2.0 – 6.5.
[f] Predicted IC50 value for blockage of HERG K+ channels. concern below −5.
[g] Predicted apparent Caco-2 cell permeability in nm/sec. Caco-2 cells are a model for the gut blood barrier. QikProp predictions are for non-active transport. <25 poor, >500 great.
[h] Prediction of binding to human serum albumin. −1.5 – 1.5.
[i] HumanO ral Absorption Predicted qualitative human oral absorption: 1, 2, or 3 for low, medium, or high. The text version is reported in the output. The assessment uses a knowledge-based set of rules, including checking for suitable values of Percent Human Oral Absorption, number of metabolites, number of rotatable bonds, logP, solubility and cell permeability.
[j] Van der Waals surface area of polar nitrogen and oxygen atoms. 7.0–200.0.

Consequently, Catechin and Linalool had the lowest and highest LUMO with energy level of −0.00150 and −0.07944, respectively. A calculation of the FMO band gap (eV) evaluated by subtracting LUMO value from HOMO value; this is particularly important because it helps to identify both the most chemically reactive compounds and most chemically inert compounds. It is well established that chemical reactivity of a molecule increases with a decrease in the energy gap, but decrease with an increase in energy gap [33]. This explanation was applied to the gap energies obtained by the compounds, and the result identify linalool as the most chemical reactive compounds in gas phase (Table 3). Catechin and Epicatechin are the least reactive compounds among the leads. The energy gap of these plants' compound may help to further explain how they interact with biomolecules including proteins.

3.6. QSAR modeling

The constructed QSAR model were used to mimics the biological activities of the plant's compounds against both aldose reductase and GSK3β. Excellent QSAR models were constructed by the AutoQSAR module of Schrodinger. The model (molprint2D_16) built for predicting the inhibitory prowess of the compounds against aldose reductase has R^2 of 0.8712, Q^2 of 0.8019, RMSE of 0.5017 (Table 4). Also, the GSK3β predictive QSAR model had R^2 of 0.7756, Q^2 of 0.8013, and RMSE of 0.5444. The scatter plots of the models are shown in Fig. 4. The details showing the predictive and observed values of the dataset for both models are listed in Table S3 and Table S4. As shown in Table 1, the pIC50 of the nine plants' compounds against both targets are satisfactory. Hence, this study demonstrated that the compounds identified as leads may exhibit excellent inhibitory attributes against these proteins when subjected to *in vivo* and in vitro investigation. Added to this, the obtained results supported some *in vivo* experiments conducted on these phytochemicals as a good antidiabetic candidate as reported by Ref. [34] amongst other scientist.

4. Conclusion

This study identified nine compounds from *S. mombin* as dual inhibitors of aldose reductase and GSK3β using molecular docking studies; and they are Quercetin, Catechin, Ellagic acid, Tangeretin, Estradiol, Epicatechin, linalool, 2-Nitroethyl benzene, and Eugenol. The compounds docking scores were validated using post-docking analysis. Through, ADME predictions, this study confirm that they showed excellent drug-like properties and pharmacokinetic values. The reactivity of the compounds in gas phase were determined, and linalool was identified as the most reactive compound. Together with the docking score, the constructed predictive QSAR showed that the nine compounds show satisfactory inhibitory effects against both aldose reductase and GSK3β. Experimental studies are ongoing to validate the findings made by this study.

Ethical approval

Not applicable.

Authors' contributions

All the authors were involved in designing, conducting, interpreting, drafting and approved of the manuscript.

Declaration of competing interest

The authors declare that they have no known competing financial interests or personal relationships that could have appeared to influence the work reported in this paper.

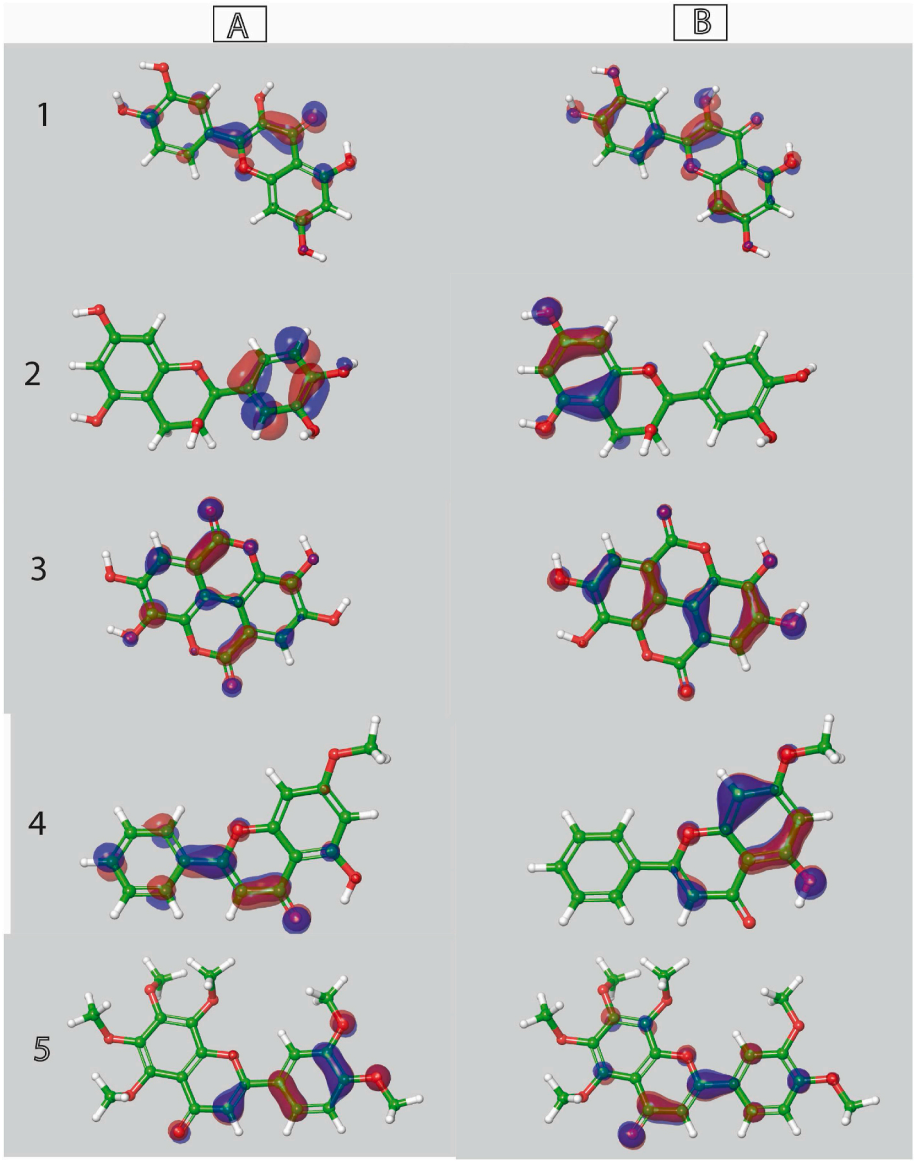

Fig. 3a. The a) HOMO and b) LUMO diagram of 1) Quercetin 2) Catechin 3) Ellagic acid 4) Tangeretin and 5) Estradiol.

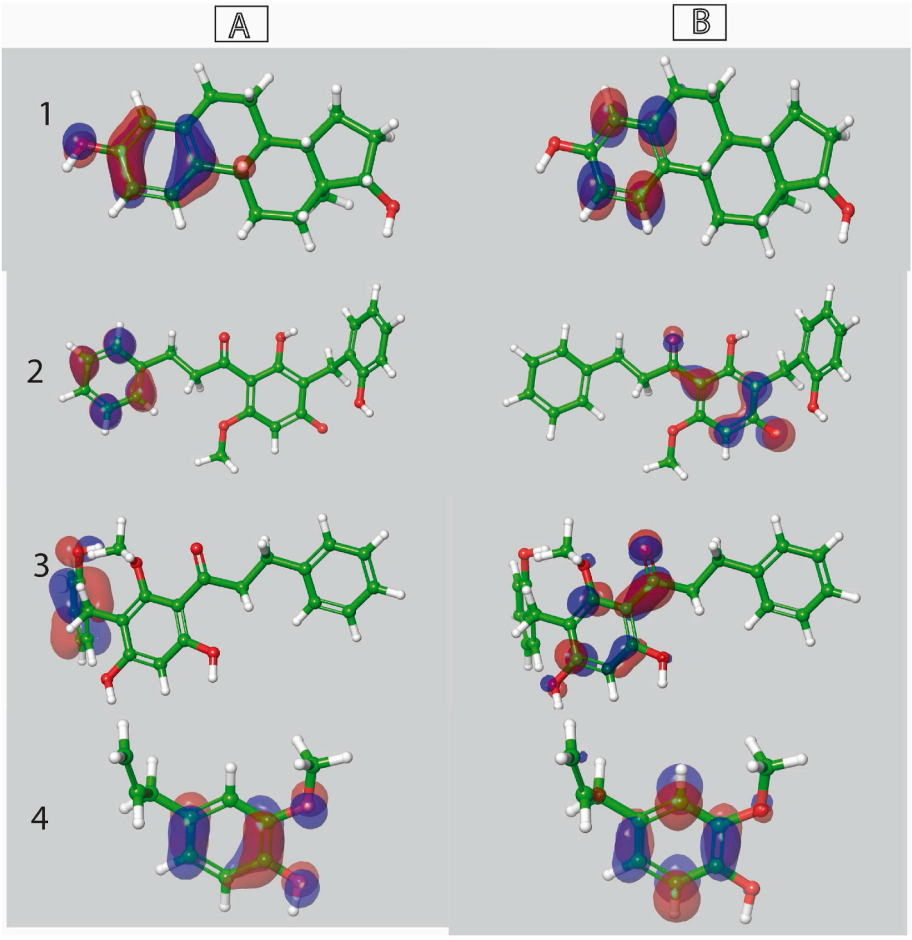

Fig. 3b. The a) HOMO and b) LUMO diagram of 1) Epicatechin 2) Linalool 3) 2-Nitroethyl benzene and 4) Eugenol.

Table 3
Calculation of frontier molecular orbital.

parameters	Quercetin	Catechin	Ellagic acid	Tangeretin	Estradiol	Epicatechin	linalool	2-Nitroethyl benzene	Eugenol
HOMO	−0.21073	−0.20630	−0.22641	−0.21888	−0.20592	−0.20710	−0.21210	−0.21669	−0.20055
LUMO	−0.05740	−0.00150	−0.07147	−0.06395	−0.05311	−0.00303	−0.09440	−0.04353	−0.00411
Band gap	−0.15333	−0.2048	−0.15494	−0.15493	−0.15281	−0.20407	−0.1177	−0.17346	−0.19644

Table 4
Best model generated for GSK-3β, Aldose reductase and GLP-1.

Parameter	Aldose reductase	GSK3β
Model code	molprint2D_16	pls_38
Score	0.792667	0.7847
S.D	0.4647	0.6662
R^2	0.8712	0.7756
RMSE	0.5017	0.5444
Q^2	0.8019	0.8013

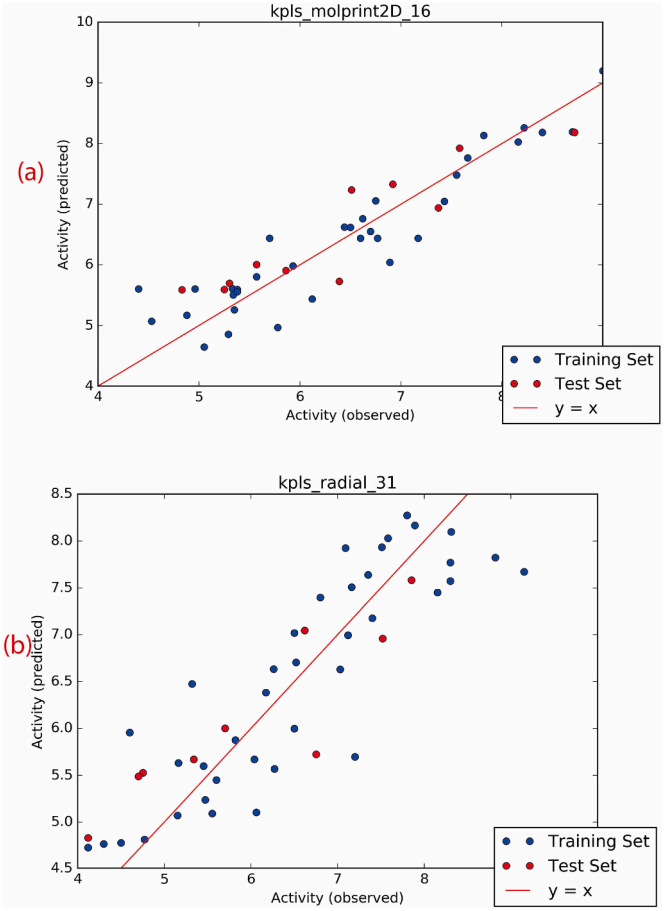

Fig. 4. Plots of a) molprint2D_ and b) Kpls_desc_38 autoQSAR model s generated from known aldose reductase and glycogen synthase kinase 3β inhibitor.

Acknowledgments

Not applicable.

Appendix A. Supplementary data

Supplementary data to this article can be found online at https://doi.org/10.1016/j.imu.2022.101126.

References

[1] Mushlin AI, Christos PJ, Abu-Raddad L, Chemaitelly H, Deleu D, Gehani AR. The importance of diabetes mellitus in the global epidemic of cardiovascular disease: the case of the state of Qatar. Trans Am Clin Climatol Assoc 2012;123:193–208.
[2] International Diabetes Federation. Diabetes atlas. eighth ed. Brussels: International Diabetes Federation; 2017.
[3] Gezawa ID, Puepet FH, Mubi BM, Uloko AE, Bakki B, Talle MA, Haliru I. Socio-demographic and anthropometric risk factors for type 2 diabetes in Maiduguri, North-Eastern Nigeria. Sahel Med J 2015;18(5):1–7.
[4] Liu J, Ren ZH, Qiang H, Wu J, Shen M, Zhang L, Lyu J. Trends in the incidence of diabetes mellitus: results from the Global Burden of Disease Study 2017 and implications for diabetes mellitus prevention. BMC Publ Health 2020;20:1415. https://doi.org/10.1186/s12889-020-09502-x.
[5] Abdi A, Jalilian M, Sarbarzeh PA, Vlaisavljevic Z. Diabetes and COVID-19: a systematic review on the current evidences. Diabetes Res Clin Pract 2020;166: 108347. https://doi.org/10.1016/j.diabres.2020.108347. Epub 2020 Jul 22. PMID: 32711003; PMCID: PMC7375314.
[6] Ramachandran A. Know the signs and symptoms of diabetes. Indian J Med Res 2014;140(5):579–81.
[7] Bacha MM, Nadeem H, Zaib S, Sarwar S, Imran A, UrRahman S, et al. Rhodanine-3-acetamide derivatives as aldose and aldehyde reductase inhibitors to treat diabetic complications: synthesis, biological evaluation, molecular docking and simulation studies. BMC Chem 2021;15(1):28. https://doi.org/10.1186/s13065-021-00756-z.
[8] Tang WH, Martin KA, Hwa J. Aldose reductase, oxidative stress, and diabetic mellitus. Front Pharmacol 2012;3:87. https://doi.org/10.3389/fphar.2012.00087.
[9] Genovese M, Imperatore C, Casertano M, Aiello A, Balestri A, Pizza L, et al. Dual targeting of PTP1B and aldose reductase with marine drug phosphoeleganin: a promising strategy for treatment of type 2 diabetes. Mar Drugs 2021;19(10):535. https://doi.org/10.3390/md19100535.
[10] Singh M, Kapoor A, Bhatnagar A. Physiological and pathological roles of aldose reductase. Metabolites 2021;11(10):655. https://doi.org/10.3390/metabo11100655.
[11] Ho EC, Lam KS, Chen YS, Yip JC, Arvindakshan M, Yamagishi S, et al. Aldose reductase-deficient mice are protected from delayed motor nerve conduction velocity, increased c-Jun NH2-terminal kinase activation, depletion of reduced glutathione, increased superoxide accumulation, and DNA damage. Diabetes 2006; 55:1946–53. https://doi.org/10.2337/db05-1497. 2006.
[12] Drel VR, Pacher P, Ali TK, Shin J, Julius U, El-Remessy AB, Obrosova IG. Aldose reductase inhibitor fidarestat counteracts diabetes-associated cataract formation, retinal oxidative-nitrosative stress, glial activation, and apoptosis. Int J Mol Med 2008;21:667–76.
[13] Maradesha T, Patil SM, Al-Mutairi KA, Ramu R, Madhunapantula SV, Alqadi T. Inhibitory effect of polyphenols from the whole green jackfruit flour against α-glucosidase, α-amylase, aldose reductase and glycation at multiple stages and their interaction: inhibition kinetics and molecular simulations. Molecules 2022;27 (6):1888. https://doi.org/10.3390/molecules27061888.
[14] Nabben M, Neumann D. GSK-3 inhibitors: anti-diabetic treatment associated with cardiac risk? Cardiovasc Drugs Ther 2016;30:233–5. https://doi.org/10.1007/s10557-016-6669-y.
[15] Wojtaszewski JFP, Hansen BF, Gade KB, Markuns JF, Goodyear LJ, Richter EA. Insulin signaling and insulin sensitivity after exercise in human skeletal muscle. Diabetes 2000;49:325–31.
[16] Eldar-Finkelman H, Krebs EG. Phosphorylation of insulin receptor substrate 1 by glycogen synthase kinase 3 impairs insulin action. Proc Natl Acad Sci USA 1997;94 (18):9660–4.
[17] MacAulay K, Woodgett JR. Targeting glycogen synthase kinase-3 (GSK-3) in the treatment of type 2 diabetes. Expert Opin Ther Targets 2008;12(10):1265–74.
[18] Bain J, McLauchlan H, Elliott M, Cohen P. The specificities of protein kinase inhibitors: an update. Biochem J 2003;371:199–204.
[19] Cabral B, Siqueira EMS, Bitencourt MAO, Lima MCJS, Lima AK, Ortmann CF, Chaves VC, Fernandes-Pedrosa MF, Rocha HAO, Scortecci KC, Reginatto FH, Giordani RB, Zucolotto SM. Phytochemical study and anti-inflammatory and antioxidant potential of Spondias mombin leaves. Revista Brasileira de Farmacognosia 2016;26:304–11.
[20] Akinmoladun AC, Adelabu AA, Saliu IO, Adetuyi AR, Olaleye MT. Protective properties of Spondias mombin Linn leaves on redox status, cholinergic dysfunction and electrolyte disturbance in cyanide-intoxicated rats. Sci Prog 2021; 104(2):1–17.
[21] Olawale F, Olofinsan K, Iwaloye O, Ologuntere TE. Phytochemicals from Nigerian medicinal plants modulate therapeutically-relevant diabetes targets: insight from computational direction. Adv Tadit Med (ADTM). 2021. https://doi.org/10.1007/s13596-021-00598-z.
[22] McConkey BJ, Sobolev V, Edelman M. The performance of current methods in ligand-protein docking. Curr Sci 2002;83:845–55.
[23] Iwaloye O, Elekofehinti OO, Oluwarotimi EA, Kikiowo BI, Fadipe TM. Insight into glycogen synthase kinase-3β inhibitory activity of phyto-constituents from *Melissa officinalis: in silico* studies. Silico Pharmacol 2020;8(1):2. https://doi.org/10.1007/s40203-020-00054-x.
[24] Ajiboye BO, Iwaloye O, Owolabi OV, Ejeje JN, Okerewa A, Johnson OO, Udebor AE, Oyinloye BE. Screening of potential antidiabetic phytochemicals from *Gongronema latifolium* leaf against therapeutic targets of type 2 diabetes mellitus: multi-targets drug design. SN Appl Sci 2022;4:14. https://doi.org/10.1007/s42452-021-04880-2. 2022.
[25] El-Kabbani O, Darmanin C, Schneider TR, Hazemann I, Ruiz F, Oka M, Joachimiak A, Schulze- Briese C, Tomizaki T, Mitschler A, Podjarny A. Ultrahigh resolution drug design. II. Atomic resolution structures of human aldose reductase holoenzyme complexed with fidarestat and minalrestat: implications for the binding of cyclic imide inhibitors. Proteins 2004;55(4):805–13.
[26] Howard EI, Sanishvili R, Cachau RE, Mitschler A, Chevrier B, Barth P, et al. Ultrahigh resolution drug design I: details of interactions in human aldose reductase-inhibitor complex at 0.66 A. Proteins 2004;1;55(4):792–804. https://doi.org/10.1002/prot.20015. PMID: 15146478.
[27] Smith E, Frenkel B. Glucocorticoids inhibit the transcriptional activity of LEF/TCF in differentiating osteoblasts in a glycogen synthase kinase-3 beta-dependent and -independent manner. J Biol Chem 2005;280:2388–94.
[28] Padavala A, Chitti S, Rajesh B, Vinukonda V, Jayanti R, Vali R. *In silico* based ligand design and docking studies of GSK-3β inhibitors. Chem Bioinform J 2010;10:1–12. https://doi.org/10.1273/cbij.10.1.
[29] Wishart DS. Improving early drug discovery through ADME modelling: an overview. Drugs R 2007;8(6):349–62. https://doi.org/10.2165/00126839-200708060-00003. PMID: 17963426.
[30] Oyinloye BE, Iwaloye O, Ajiboye BO. Polypharmacology of *Gongronema latifolium* leaf secondary metabolites against protein kinases implicated in Parkinson's disease and Alzheimer's disease. Scientific African 2021;12(3):e00826. https://doi.org/10.1016/j.sciaf.2021.e00826.
[31] Lipinski CA, Lombardo F, Dominy BW, Feeney PJ. Experimental and computational approaches to estimate solubility and permeability in drug discovery and development settings. Adv Drug Deliv Rev 2001;46(1–3):3–26.
[32] Iwaloye O, Elekofehinti OO, Olawale F, Chukwuemeka OP, Babatomiwa K, Folorunso MI. Fragment-Based Drug Design, 2D-QSAR and DFT Calculation: scaffolds of 1, 2, 4, triazolo [1, 5-a] pyrimidin-7-amines as potential inhibitors of

Plasmodium falciparum dihydroorotate dehydrogenase. Lett Drug Des Discov 2022;19. https://doi.org/10.2174/1570180819666220422120707.

[33] Olawale F, Iwaloye O, Olofinsan K, Ogunyemi OM, Gyebi GA, Ibrahim IM. Homology modelling, vHTS, pharmacophore, molecular docking and molecular dynamics studies for the identification of natural compound-derived inhibitor of MRP3 in acute leukaemia treatment. Chem Pap 2022;2022a. https://doi.org/10.1007/s11696-022-02128-w.

[34] Shabbir U, Rubab M, Daliri EBM, Chelliah R, Javed A, Oh DH. Curcumin, Quercetin, catechins and metabolic diseases: the role of gut microbiota. Nutrients 2021;13:206. https://doi.org/10.3390/nu13010206.